Journal of Aerosol Science 159 (2022) 105878

Contents lists available at ScienceDirect

Journal of Aerosol Science

journal homepage: www.elsevier.com/locate/jaerosci

Towards a concentration closure of sub-6 nm aerosol particles and sub-3 nm atmospheric clusters

Markku Kulmala [a,b,c,d], Dominik Stolzenburg [a,*], Lubna Dada [a,e,f], Runlong Cai [a], Jenni Kontkanen [a], Chao Yan [a,b], Juha Kangasluoma [a], Lauri R. Ahonen [a], Loïc Gonzalez-Carracedo [g], Juha Sulo [a], Santeri Tuovinen [a], Chenjuan Deng [h], Yiran Li [h], Katrianne Lehtipalo [a,i], Kari E.J. Lehtinen [j], Tuukka Petäjä [a,c], Paul M. Winkler [g], Jingkun Jiang [h], Veli-Matti Kerminen [a,c]

[a] Institute for Atmospheric and Earth System Research (INAR) / Physics, Faculty of Science, University of Helsinki, Finland
[b] Aerosol and Haze Laboratory, Beijing Advanced Innovation Center for Soft Matter Sciences and Engineering, Beijing University of Chemical Technology (BUCT), Beijing, China
[c] Joint International Research Laboratory of Atmospheric and Earth System Sciences, School of Atmospheric Sciences, Nanjing University, Nanjing, China
[d] Faculty of Geography, Lomonosov Moscow State University, Moscow, Russia
[e] EPFL, School of Architecture, Civil and Environmental Engineering, Sion, 1951, Switzerland
[f] Laboratory of Atmospheric Chemistry, Paul Scherrer Institute, Villigen, Switzerland
[g] Faculty of Physics, University of Vienna, Vienna, Austria
[h] State Key Joint Laboratory of Environment Simulation and Pollution Control, School of Environment, Tsinghua University, Beijing, China
[i] Finnish Meteorological Institute, Erik Palménin Aukio 1, 00560, Helsinki, Finland
[j] Department of Applied Physics, University of Eastern Finland and Finnish Meteorological Institute, Kuopio, Finland

ARTICLE INFO

Keywords:
New particle formation
Atmospheric clusters
Particle number concentrations
Urban environment
Boreal forest
Sub-10 nm

ABSTRACT

Atmospheric clusters play a key role in atmospheric new particle formation and they are a sensitive indicator for atmospheric chemistry. Both the formation and loss of atmospheric clusters include a complex set of interlinked physical and chemical processes, and therefore their dynamics is highly non-linear. Here we derive a set of simple equations to estimate the atmospheric cluster concentrations in size ranges of 1.5–2 nm and 2–3 nm as well as 3–6 nm aerosol particles. We compared the estimated concentrations with measured ones both in a boreal forest site (the SMEAR II station in Hyytiälä, Finland) and in an urban site (the AHL/BUCT station in Beijing, China). We made this comparison first for 3–6 nm particles, since in this size range observations are more reliable than at smaller sizes, and then repeated it for the 2–3 nm size range. Finally, we estimated cluster concentrations in the 1.5–2 nm size range. Our main finding is that the present observations are able to detect a major fraction of existing atmospheric clusters.

1. Introduction

New particle formation (NPF) is both a globally occurring and a frequent phenomenon in the Earth's lower atmosphere (e.g. Chu

* Corresponding author.
E-mail address: dominik.stolzenburg@helsinki.fi (D. Stolzenburg).

https://doi.org/10.1016/j.jaerosci.2021.105878
Received 16 June 2021; Received in revised form 20 September 2021; Accepted 20 September 2021
Available online 24 September 2021

et al., 2019; Kerminen et al., 2018; Kulmala et al., 2004). As outlined by Kulmala et al. (2014), atmospheric NPF is a multi-step process starting from molecular cluster formation and eventually leading to a growing aerosol particle population. When reaching larger sizes, particles originating from atmospheric NPF may have significant influences on the global cloud condensation nuclei budget (e.g. Gordon et al., 2017), human health (Ohlwein et al., 2019) and even haze formation in heavily-polluted environments (Guo et al., 2014; Kulmala et al., 2021).

Recent progress in measurement methods and theoretical understanding, together with their application in laboratory and field conditions, have brought extensive new insights into atmospheric NPF. More specifically, we start to have detailed information on the composition of the smallest, sub-1.5 nm atmospheric charged clusters, and this knowledge has revealed the diversity of cluster formation mechanisms in different atmospheric environments (Beck et al., 2021; Bianchi et al., 2021; Brean et al., 2021; Cai et al., 2021; Jokinen et al., 2018; Lehtipalo et al., 2018; Sipilä et al., 2016; Yan et al., 2021; Yao et al., 2018). At the same time, we have accumulated plenty of information on atmospheric NPF events in terms of their frequency of occurrence, and the associated particle formation and growth rates at sizes larger than 3 nm of the particle diameter (Chu et al., 2019; Kerminen et al., 2018). What is missing is the exact connection between the molecular clusters and atmospheric NPF events, making it difficult to quantify the link between emissions of aerosol precursors and potential influences of atmospheric NPF on climate or human health. A key factor towards building this connection is to understand the properties of 1.5–3 nm atmospheric clusters, including their concentration in different environments.

The continuous presence of sub-2 nm ions in the atmosphere has been known already for decades (e.g. Tammet, 1995; Manninen et al., 2010; Hirsikko et al., 2011 and references therein). Kulmala et al. (2000) predicted theoretically that also electrically neutral sub-3 nm clusters exist but, due to the lack of a technique to detect them, this could not be verified for several years. The first atmospheric measurements showing the continuous presence (including NPF and non-NPF times) of sub-3 nm neutral clusters were performed at the SMEAR II station in a boreal forest environment by utilizing a Neutral cluster and Air Ion Spectrometer (NAIS) and Condensation Particle Counters (CPCs) able to detect ~2–3 nm neutral particles (Kulmala et al., 2007; Sipilä et al., 2008; Lehtipalo et al., 2009, 2010). After that, the development of CPCs using diethylene glycol (DEG) as their working fluid has enabled the detection of neutral clusters down to ~1 nm sizes (Iida et al., 2009; Jiang, Chen, et al., 2011; Vanhanen et al., 2011; Wimmer et al., 2013). The most commonly used DEG-based instruments are the Particle Size Magnifier (PSM; Vanhanen et al., 2011) and DEG-SMPS (Jiang, Chen, et al., 2011) which both can measure the size distribution of particles in the ~1–3 nm size range.

Using the instruments outlined above, sub-3 nm clusters have been observed in vastly different environments, including the boreal forest (Dada et al., 2018; Kulmala et al., 2013; Manninen et al., 2009; Rose et al., 2018), mountain sites (Rose et al., 2015; Bianchi et al., 2016, 2021), megacities (Cai et al., 2017a; Kulmala et al., 2021; Xiao et al., 2015; Yu et al., 2016; Deng et al., 2020; Zhou et al., 2020), other urban environments (Jiang, Zhao, et al., 2011; Kontkanen et al., 2017; Yu et al., 2016), coastal areas (Yu et al., 2014; Sipilä et al., 2016), and rural sites (Kontkanen et al., 2016). Typical concentrations of sub-3 nm clusters have been found to range from a few hundred to about 100 000 cm^{-3} in different environments, noting that the measured size range has been slightly different at the different sites. The highest concentrations have been detected in polluted urban environments (Deng et al., 2021), and the lowest ones in clean environments such as high-altitude sites. The recent study by Sulo et al. (2021) reported a median sub-3 nm cluster concentration of about 400 cm^{-3} in a boreal forest environment, which is similar to earlier observations at several sites in the United States (Kontkanen et al., 2017; Yu et al., 2014).

Despite the increasing number of observations of sub-3 nm atmospheric clusters, the uncertainties in these measurements are still large (Kangasluoma et al., 2020; Kangasluoma & Kontkanen, 2017). These uncertainties originate from various sources, such as high sampling losses of small particles and the effects of particle chemical composition, particle charging state and environmental conditions on the detection efficiency of the instruments (Jiang, Chen, et al., 2011; Kangasluoma et al, 2013, 2016). However, recent advances in electrical mobility spectrometry (Brilke et al., 2020; Cai et al., 2017; Fu et al., 2019; Stolzenburg et al., 2017) allow for new insights into cluster concentrations with an unprecedented precision.

The primary goal of this paper is to find out how reliable present-day observations of sub-3 nm clusters are, and whether some or even a major fraction of such clusters cannot be detected using the current measurement instruments. Previous attempts to bring molecular cluster measurements with particle size-distributions into agreement have been pursued in e.g. Kulmala et al. (2013) and Jiang, Zhao, et al. (2011). Now, we approach the problem by combining observations with theoretical calculations to investigate how good a closure we can obtain between the measured and predicted cluster concentrations in different size ranges in atmospheric environments. We start with investigating how good the steady-state approximation to calculate cluster concentrations is in practice. Then we investigate the closure. For that purpose, we utilize observations from two vastly different environments: Hyytiälä in Finland and Beijing in China. We first compare measured and estimated concentrations of 3–6 nm particles, since in this size range observations are more reliable than those at smaller sizes. Then we repeat this comparison in the 2–3 nm size range, and finally estimate 1.5–2 nm cluster concentrations in these environments.

2. Towards a cluster closure

In order to obtain a closure of cluster concentrations, we will perform conceptual calculations. First, we will derive an expression for the number concentrations of clusters in a specific size range from the balance between the cluster formation rates and sinks.

We start with the balance equation that determines the concentration of clusters in the diameter range of 2–3 nm, $N_{2\text{-}3}$:

$$\frac{dN_{2-3}}{dt} = J_2 - J_3 - N_{2-3} \cdot \mathrm{CoagS}_{2-3} \quad (1)$$

Here J_2 is the formation rate of 2-nm clusters, i.e. the cluster flux into the 2–3 nm size range, J_3 is formation rate of 3-nm clusters, i.e. the flux of clusters out of this size range due to their growth, and $CoagS_{2\text{-}3}$ is the coagulation sink of 2–3 nm clusters, i.e. the rate at which 2–3 nm clusters are scavenged by coagulation with larger pre-existing particles. Equation (1) is obtained by integrating the aerosol general dynamic equation (GDE), that includes condensation and coagulation loss terms, from 2 to 3 nm.

Next, we assume a pseudo steady state between the sources and sinks of 2–3 nm clusters by approximating $dN_{2\text{-}3}/dt = 0$ in equation (1), after which we get:

$$N_{2-3} = \frac{J_2 - J_3}{\mathrm{CoagS}_{2-3}} \tag{2}$$

where J_2, J_3 and $CoagS_{2\text{-}3}$ are calculated from observations (see, e.g. Kulmala et al., 2012). By comparing the measured number concentrations with the values calculated using equation (2), we can find out how good assumption the pseudo steady state is, and whether we have all crucial phenomena included in our equations.

The formation rates J_2 and J_3 can also be related to each other following Kerminen and Kulmala (2002):

$$J_3 = J_2 \cdot e^{-a} \tag{3a}$$

$$J_2 = J_3 \cdot e^{a} \tag{3b}$$

where

$$a = 0.23 \cdot \left(\frac{1}{d_1} - \frac{1}{d_2}\right) \cdot \mathrm{CS}' \Big/ \mathrm{GR} \tag{4}$$

Here, d_1 and d_2 are the lower and upper diameters of the considered size range given in the unit nm (here 2 nm and 3 nm, respectively), GR is the growth rate of 2–3 nm clusters in nm/h, and $CS' = CS/(4\pi D_{H2SO4}) \approx CS \times 10^4$ is the condensation sink in 10^4 s^{-1}, calculated for a sulfuric acid monomer. The Kerminen-Kulmala equations, 3a and 3b, assume that GR is constant and $CS \sim dp^{-2}$ in the size range 2–3 nm.

As a result, $N_{2\text{-}3}$ can also be expressed as

$$N_{2-3} = J_3 \cdot (e^a - 1)/\mathrm{CoagS}_{2-3} \tag{5}$$

If we further approximate GR in the size range 2–3 nm with GR determined for 3 nm or slightly above, equation (5) allows us to estimate $N_{2\text{-}3}$ using measurement data solely from sizes larger than 3 nm of the particle diameter.

Note that the pseudo-steady state assumption made in deriving equation (5) may break down under conditions of very rapidly changing cluster sinks or sources. In such cases, equation (1) needs to be solved numerically in order to obtain $N_{2\text{-}3}$.

The equations given above concern the size range of 2–3 nm. We can derive similar equations for any other size range, such 3–6 nm or 1.5–2 nm to obtain $N_{3\text{-}6}$ and $N_{1.5\text{-}2}$, respectively, simply by replacing the relevant quantities (J, CoagS) with those inherent for that size range. Note that the coagulation sink of clusters or particles at any size or size range can be obtained from the condensation sink (CS) using the equation derived by Lehtinen et al. (2007):

$$CoagS(D_p) = CS \cdot \left[\frac{0.71}{D_p}\right]^n \tag{6}$$

where n is typically between about 1.5 and 2 depending on the particle number size distribution.

In the calculations of this work, we assumed $n = 1.6$ in equation (6), which is a typical value of n for SMEAR II data (Lehtinen et al., 2007), whereas in equation (4) it has implicitly been assumed that $n = 2$. The influences of coagulation scavenging on cluster concentrations are, however, not very sensitive to the exact value of this parameter. When calculating CoagS for any size range [d_1, d_2] using equation (6), we set D_p equal to the geometric mean of d_1 and d_2.

The formation rates were calculated from the measured particle number size distributions and their corresponding change rates as in Kulmala et al. (2012):

$$J_{d_1} = \frac{dN_{[d_1,d_2]}}{dt} + CoagS_{[d_1,d_2]}N_{[d_1,d_2]} + \frac{\mathrm{GR}}{(d_2 - d_1)}N_{[d_1,d_2]} \tag{7}$$

where d_1 is the size at which the formation rate is calculated, and d_2 is the upper interval bound for which the change rate of the particle or cluster number concentration is calculated. Here, in line with the common terminology used in the earlier literature, we call the particle formation rate calculated using equation (7) as the "measured" particle formation rate. In calculating J_2, J_3 and J_6, we used 2, 3, and 6 nm for d_1 and 4, 6, and 10 nm for d_2, respectively. For GR we used the corresponding observed value at each day obtained via the maximum concentration method (e.g. Kulmala et al., 2012), which might also introduce some error, as the conditions when growth is measured might not be representative for the entire day, especially nighttime. Therefore, the lower error bounds on the formation rates and all subsequent calculations include the effect of GR = 0 during nighttime. Note that the growth term for the formation rate calculations in Beijing is very minor, and the assumption of GR = 0 during nighttime barely affects the error estimate.

3. Results and discussion

3.1. Cluster mode

It has been known for decades that there is a constantly existing mode of small ions (sub-2 nm), and that the somewhat larger intermediate ions exist typically only during NPF events (e.g. Hirsikko et al., 2011; Manninen et al., 2010; Tammet, 1995). Kulmala et al. (2000) suggested based on their theoretical calculations that there is also a mode of neutral clusters in sub-3 nm size range. Based on the observations, we can state that there is always a cluster mode present in the atmosphere (e.g. Kontkanen et al., 2017; Kulmala et al., 2013; Manninen et al., 2010; Zhou et al., 2020). Often particle or cluster number concentrations in this mode are higher than those in the nucleation, Aitken or accumulation modes, or in all those three modes together. Therefore, we suggest that the representations of sub-micron atmospheric aerosols include a cluster mode (Fig. 1).

3.2. Towards a closure between observations and calculations

In spite of the present progress in observations of sub-3 nm particle size distributions and concentrations, it is still hard to observe exact concentrations in the sub-2 nm size range when these concentrations are low. Therefore, we look here at the closures in the 2–3 nm size range based on observations at the SMEAR II station in Hyytiälä, Finland (Hari & Kulmala, 2005), and also in AHL/BUCT laboratory in Beijing, China (Liu et al., 2020). As a comparison, we have also investigated the closures in the size range of 3–6 nm.

The measurements were performed using a DMA-train (Stolzenburg et al., 2017) at SMEAR II station in Hyytiälä, Finland, (e.g. Hari & Kulmala, 2005; Kulmala et al., 2013) and a DEG-SMPS equipped with the improved DMA and sampling inlet (Cai et al., 2017a; Fu et al., 2019; Jiang, Chen, et al., 2011) at the AHL/BUCT station in Beijing, China (e.g. Liu et al., 2020). Both instruments rely on electrical mobility analyzers for obtaining the sizing information. Besides their lower sensitivity towards small particle number concentrations compared to the PSM, the better sizing accuracy provides more stable estimates of number concentrations in the 2–3 nm size range. Furthermore, they additionally yield information at bigger sizes, such that we can compare our cluster closure over a

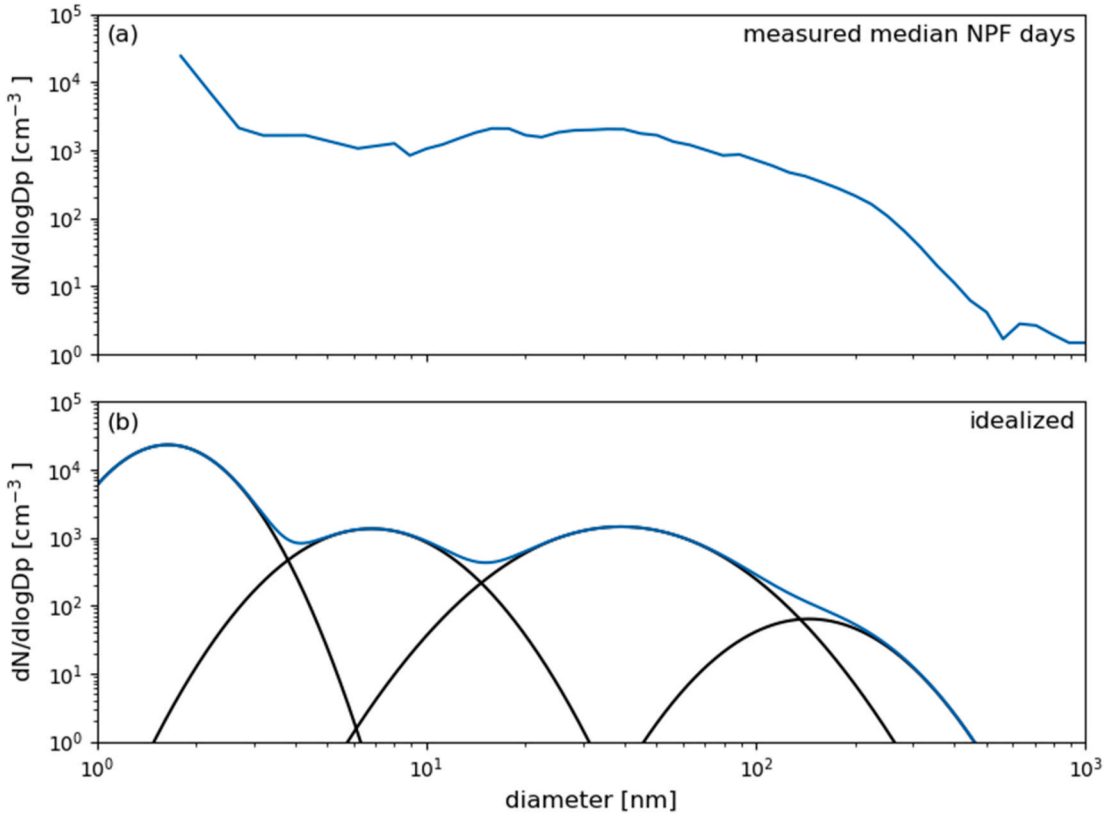

Fig. 1. A schematic number size distributions including cluster mode based on the median values observed at SMEAR II station in Hyytiälä, spring 2020, NPF days, daytime (8 a.m.-16 p.m.). (a) Measured number size distribution obtained from a DMA-train (Stolzenburg et al., 2017) and a twin-differential mobility particle sizer system (Aalto et al., 2001). (b) A typical idealized distribution including four lognormal modes is shown. This includes a cluster mode (sub−3 nm), which is usually measured using a particle size magnifier (Vanhanen et al., 2011), the nucleation mode (3–25 nm) measured using a Neutral and Air ion Spectrometer in total mode (Mirme & Mirme, 2013), and an Aitken mode (25–100 nm) and Accumulation mode (100–1000 nm), which are routinely measured using a twin-DMPS (Aalto et al., 2001).

larger size-range with the same instrumentation.

In Fig. 2a we show the observed diurnal variation of formations rates (J_2, J_3, and J_6) at the SMEAR II station, and in Fig. 2b the corresponding values at the AHL/BUCT station, for NPF days in the spring/summer periods of 2020 (SMEAR II) and 2018 (AHL/BUCT). The compared datasets cover roughly five months and are representatives for typical NPF conditions at both sites. Fig. 2 demonstrates that the formation rates are typically 50–100 times higher in Beijing than in Hyytiälä at all the calculated sizes.

In Fig. 3, we show the values of condensation and coagulation sinks in both sites during the NPF days, as determined using Eq. (6). Overall, the values of both CS and CoagS were roughly a factor of 10 higher in Beijing than in Hyytiälä. On the contrary, as shown Fig. 4, growth rates were pretty similar at both sites. This is consistent with previous studies (e.g. Kerminen et al., 2018; Kulmala et al., 2004). The growth rates showed a clear increase with an increasing particle size, which has been previously observed at the same sites and in many other environments, to be a typical feature as well (e.g. Deng et al., 2020; Kuang et al., 2012; Kulmala et al., 2013). Together with observed sink values, the observed growth rates were used to calculate the theoretically estimated particle formation rates using the Kerminen & Kulmala equation (Eq. (3b)) and subsequently cluster concentrations using Eq. (5).

In Fig. 5 we start by comparing the estimated and measured diurnal variations of particle formation rates and number concentrations in the range of 3–6 nm, where instrument-related measurement uncertainties are lower. The estimated diurnal median particle concentrations using Eq. (2) and the measured values agree nicely for Hyytiälä and Beijing daytime, as shown in Fig. 5a and b. Note that for Beijing we expect a significant contribution of primary emissions at the BUCT/AHL station (Kontkanen et al., 2020) for the size interval of interest. In order to reduce the influence of primary emissions on Eq. (2), which scales linearly with the difference J_{d1}-J_{d2} of two formation rates, we used 25 nm as the upper interval bound d_2 for the calculation of J_2, J_3 and J_6 in Beijing, as shown in Fig. S1 in the Supplement. By taking the larger size interval, the increasing primary emissions at larger sizes are offsetting both formation rate calculations, reducing the influence on the calculated difference. However, in terms of absolute numbers the calculated values of J_2, J_3, J_6 would be less accurate using this larger size interval. Fig. S1 shows that the adjustment of the formation rate calculation increases the accuracy of using Eq. (2) for Beijing, especially during afternoon and nighttime, where primary emissions might dominate the dN/dt term in the formation rate calculation of Eq. (7).

With the approach of Eq. (2), the estimated and measured values are highly coupled, as the same size-distribution information is used for calculating the formation rates at 3 and 6 nm and the concentration estimate for that size-range. However, the results given in Fig. 5a and b using equation (2) confirm that we have included all the relevant processes in our expressions and that the pseudo steady state approximation is valid. In Fig. 5c and d we show J_3 estimated using J_6 and the Kerminen & Kulmala equation (Eq. (3b)), together with measured values of J_3 obtained using equation (7), for both sites. Especially during daytime, we also obtain agreement within the uncertainties for both methods and both locations. This then further translates into some overlap for the predicted number concentrations using Eq. (5), as shown in Fig. 5e and f, however the agreement gets slightly worse, especially for Hyytiälä. Here Eq. (5) is used as an independent test of a closure between the observed and predicted values (Fig. 5e and f), since the estimated values do not rely on any measurements below 6 nm. It needs to be noted that approximating the GR in Eq. (5) using measurements at larger sizes introduces an underestimation of the number concentration due to typically increasing GR with size (Fig. 4). Moreover, the results are generally extremely sensitive to quantities like the GR and CS, which can usually have high systematic uncertainties (e.g. Leppä et al., 2011; Yli-Juuti et al., 2011; Kulmala et al., 2017).

The same procedure is now repeated for the more challenging size range of 2–3 nm. In Fig. 6 we show again the comparisons between estimations and measurements using Eq. (2) (Fig. 6a and b), and the estimates using the Kerminen & Kulmala equation for the particle formation rates (Fig. 6c and d) and cluster concentrations (Fig. 6e and f). The agreement using Eq. (2) is again remarkable for both sites (again especially when reducing the influence of primary emissions in Beijing by changing the intervals for the nucleation rate calculations as shown in Fig. S2) and well within the uncertainties (estimated by the $25^{th}/75^{th}$ quantiles of both the nucleation rate and CoagS measurements for the predicted values). Using the Kerminen & Kulmala equation we can also reproduce the particle formation rates at 2 nm within the error bars (estimated using the $25^{th}/75^{th}$ quantiles for CS and GR in the Kerminen & Kulmala estimate). As pointed out above, the approximation of the GR with the measurement from larger size range induces a systematic underestimation of cluster concentrations. However, GR is often known from either literature or can be inferred by a different set of

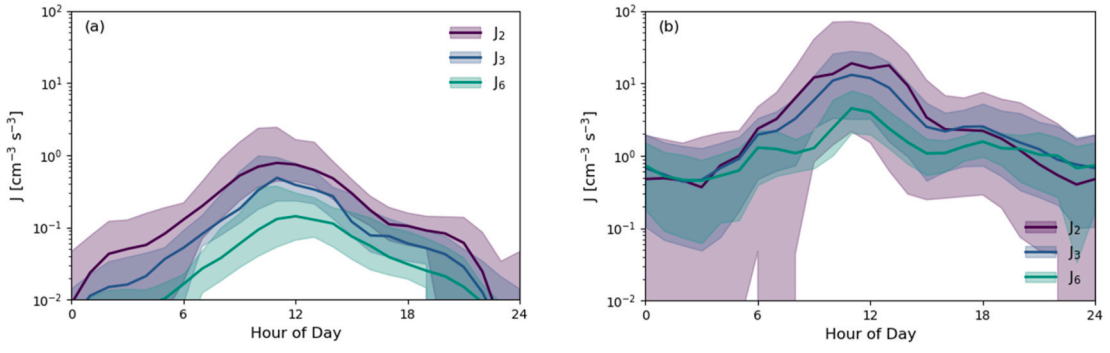

Fig. 2. Formation rates (J_2, J_3 and J_6 calculated based on the size intervals of 2–4, 3–6 and 6–10 nm, respectively) during NPF event days at SMEAR II station in Hyytiälä, Finland (a) and at AHL/BUCT station Beijing China (b). Median (lines) as well 25% and 75% quartiles are presented.

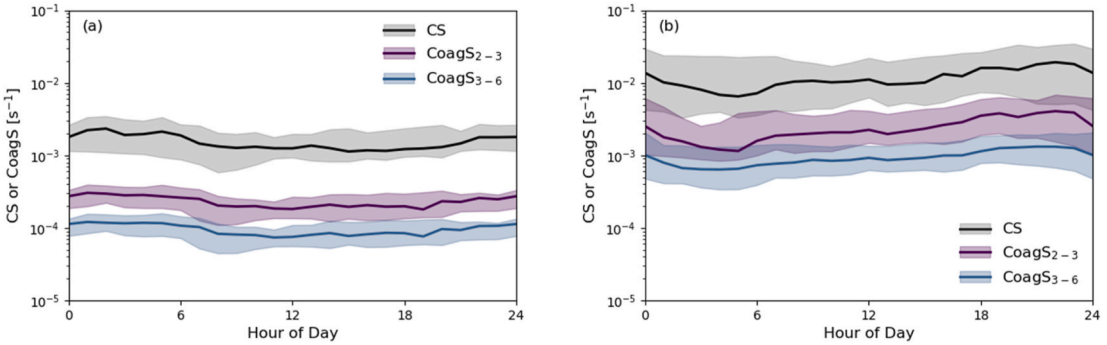

Fig. 3. Diurnal variations of condensation or coagulations sinks in Hyytiälä (a) and Beijing (b) during NPF event days.

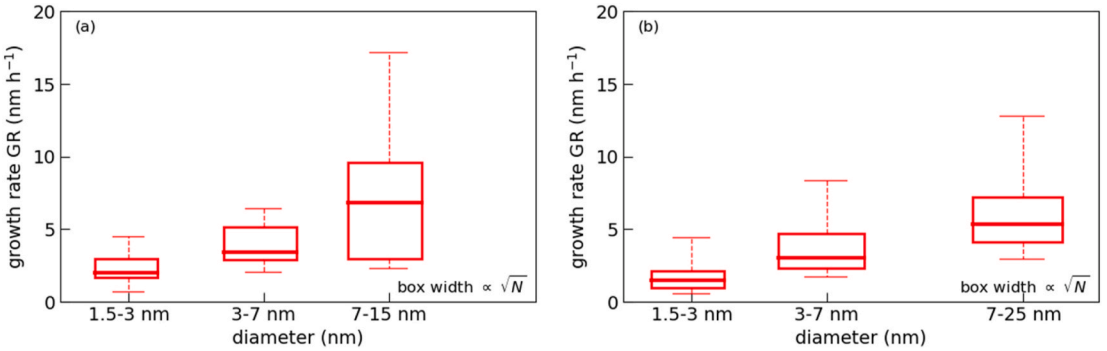

Fig. 4. Particle growth rates as a function of size. In Hyytiälä, 2020 (a) and in Beijing, 2018 (b).

instrumentation than used for the number concentration measurements (e.g. NAIS ion GR). Therefore, without circular deduction, values from Kulmala et al. (2013) and Deng et al. (2020) are used in Figs. S3 and S4 in the Supplement giving better agreement for Hyytiälä and a slight overestimation of cluster concentrations in Beijing. The higher values in Beijing are in line with the investigations of Kulmala et al. (2017) explaining that the effective sink could actually be much smaller than the observed one (see also Tuovinen et al., 2020). Again, these small deviations between the estimated and measured formation rates at 2 nm translate into stronger deviations for the cluster concentrations (Fig. 6e and f). Nevertheless, we show that our measurements and estimations are within the same order of magnitude for two complimentary sites, indicating the presence of a strong cluster mode during new particle formation.

Additionally, our estimates of the cluster concentrations in Hyytiälä are clearly higher than those measured by Sulo et al. (2021) at the same site and those reported by some other earlier studies. This indicates significant differences in the used methodology, e.g. systematic biases between the instruments. These biases are probably related to the measurement method (the PSM sizing relies on activation-equivalent diameters) as well as different assumptions used in the calculations. We demonstrated above that the predicted cluster concentrations are very sensitive to the ratio of condensation sink to growth rate (CS/GR). As discussed by Kulmala et al. (2017) and Tuovinen et al. (2020), this ratio could be overestimated in polluted environments.

To underline the value of the cluster closure analysis, we explored the published data set from Hyytiälä, Finland (Kulmala et al., 2013). According to Kulmala et al. (2013), the median particle growth rates in the size ranges of 1.5–2 nm, 2–3 nm and 3–5 nm were 0.9, 2.1 and 2.7 nm h^{-1}, respectively, while CS had a clear diurnal variation during the NPF days between about 0.001 and 0.003 s^{-1}. The observed formation rates were (typical noon maximum values) 3, 1.5 and 0.4 cm^{-3} s^{-1} at 1.5, 2.0 and 3.0 nm, respectively. Using these values with CS = 0.003 s^{-1} together with equation (3b), we get $J_2 = 1.7 \times J_3$ and $J_{1.5} = 3.6 \times J_2$. We also calculated $J_{1.5}$ as a function of J_3 and obtained $J_{1.5} = 2.5$ cm^{-3} s^{-1}. This value is within 20% of the observed $J_{1.5}$. The estimated cluster number concentration (Eq (5)) in size range of 1.5–2.0 nm is 2300–7900 cm^{-3}, while the measured one was 3000 cm^{-3} (Kulmala et al., 2013). Therefore, the closure for the cluster concentrations is a valuable tool to estimate the feasibility of the measured cluster number concentrations. This is particularly important in the size range that is at the same time challenging to measure and prone to considerable uncertainty and sensitive to e.g. sampling losses.

3.3. Sensitivity of estimated cluster concentrations

Using the closure equations, which were shown to work at least as order of magnitude estimates for the size ranges above 3 nm, we can investigate order of magnitude concentrations of clusters of different sizes. Here we make such estimates for the cluster sizes of 1.5–2.0 nm and 2.0–3.0 nm.

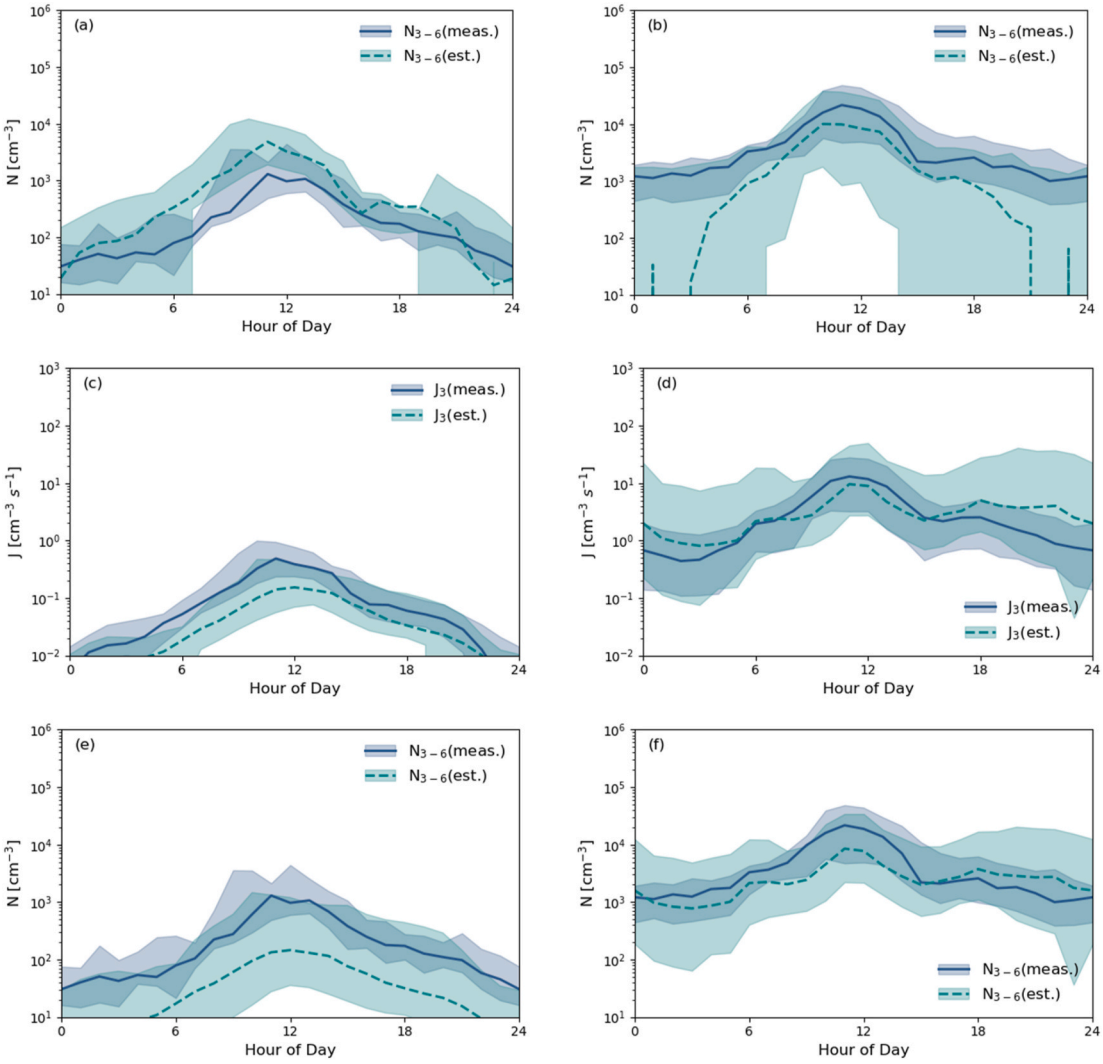

Fig. 5. Measured and estimated median diurnal number concentrations of 3–6 nm particles and particle formation rates at 3 nm. (a) and (b) show the measured (solid line) and according to Eq. (2) (dashed line) the estimated values of $N_{3\text{-}6}$ for Hyytiälä and Beijing, respectively. (c) and (d) show the measured (solid line) and estimated according to Eq. (3b) (dashed lines) values of J_3 for Hyytiälä and Beijing, respectively. (e) and (f) show the measured and estimated according to Eq. (5) values of $N_{3\text{-}6}$ for Hyytiälä and Beijing, respectively. The shaded areas show the 25–75 quantile for all values.However, the lower error bound for nighttime is estimated from the 25th percentile of the data assuming GR = 0 in the formation rate calculations.

In Fig. 7 we show the cluster concentration scaled by the J calculated from equations (2), (3) and (5) as a function of CS/GR. This underlines the sensitivity of the ratio N/J to the ratio CS/GR.

The dependency of particle formation rate at 2 and 3 nm on the cluster concentrations (1.5–2 and 2–3 nm) is linear. Therefore, by using the typical values for J_2, CS and GR in Beijing and Hyytiälä we can estimate that $N_{1.5\text{–}2}$ is about 50 000–200 000 cm^{-3} in Beijing and about 1500–10000 cm^{-3} in Hyytiälä. Since CS/GR is a factor of 10 higher in Beijing than in Hyytiälä and formation rates are also a factor of 10–20 higher in Beijing than in Hyytiälä, the estimated number concentrations are a factor of 10–100 higher. However, in both places but particularly in Beijing, the estimated cluster concentrations are very sensitive to CS/GR.

4. Conclusions

During the recent years, the knowledge on atmospheric cluster concentrations has been increasing significantly (e.g. Kulmala et al., 2017, 2021; Yu et al., 2014, 2013; Kontkanen et al., 2017, 2016; Yu et al., 2016; Zhou et al., 2020; Sulo et al., 2021), demonstrating the ubiquitous presence of a cluster mode with high concentrations – exceeding significantly the ion concentrations - in different atmospheric environments. In this paper, we derived a simple conceptual model. Using this model, we were able to show that a) that the pseudo-steady state approximation is valid in the studied conditions and b) that the measured cluster concentrations in the 2–3 nm size

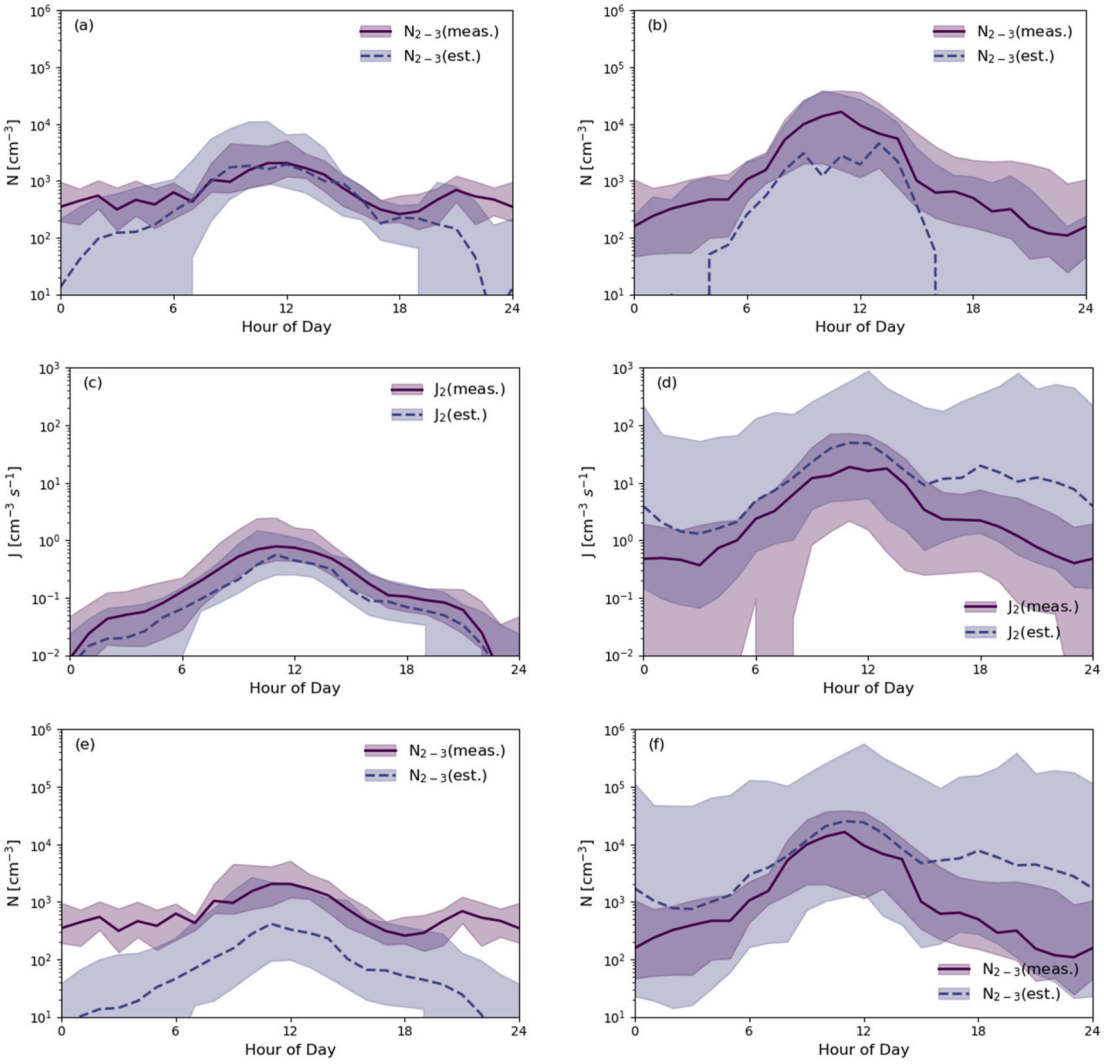

Fig. 6. Measured and estimated median diurnal number concentrations 2–3 nm clusters and particle formation rates at 2 nm. (a) and (b) show the measured (solid line) and according to Eq. (2) (dashed line) the estimated values of $N_{2\text{-}3}$ for Hyytiälä and Beijing, respectively. (c) and (d) show the measured (solid line) and estimated according to Eq. (3b) (dashed lines) values of J_2 for Hyytiälä and Beijing, respectively. (e) and (f) show the measured and estimated according to Eq. (5) values of $N_{2\text{-}3}$ for Hyytiälä and Beijing, respectively. The shaded areas show the 25–75 quantile for all values. However, the lower error bound for nighttime is estimated from the 25th percentile of the data assuming GR = 0 in the formation rate calculations.

range agree with the estimated ones typically within a factor of 2–10. Since the aim of this conceptual model development is to provide a tool for an order-of-magnitude estimation of atmospheric cluster concentrations, its predictions can be considered relatively accurate for this purpose.

Furthermore, based on model predictions we showed that the cluster concentrations in both 1.5–2 nm and 2–3 nm size range depend strongly on the cluster growth rate and coagulation sink in this size range. Also, the concentrations depended linearly on the formation rate at 1.5, 2 or 3 nm regardless of whether we calculated it forwards (from 1.5 to 2 nm or from 2 to 3 nm) or backwards (from 3 to 2 nm or from 2 to 1.5 nm). The estimated cluster concentrations were on the order of 1000–10 000 cm^{-3} in the 1.5–2 nm size range in a background site like Hyytiälä in Finland and 10–100 times higher in polluted megacities like in Beijing, China.

By comparing cluster concentrations based on the calculated closure with measured ones, we can conclude that the present observation techniques typically are able to detect a major fraction of existing atmospheric clusters at least within the order of magnitude. However, we still need to improve the accuracy of detection of sub-3 nm clusters, since present uncertainties remain to be large.

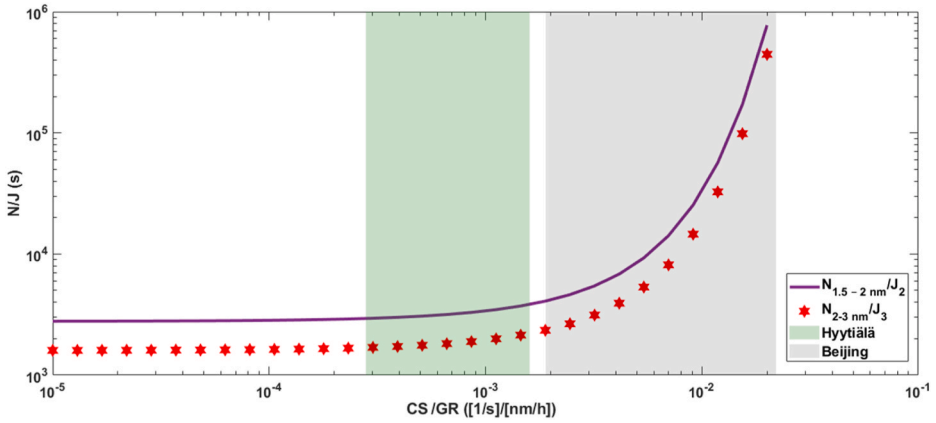

Fig. 7. Concentration of clusters (1.5–2 nm) scaled with the formation rate at 2 nm marked with red stars, and concentrations of clusters (2–3 nm) scaled with the formation rate at 3 nm (blue line), as a function of CS/GR at the corresponding size range. The differences between the two curves (in N/J) is mainly due to the fact that CoagS is smaller for 2–3 nm clusters than for 1.5–2 nm clusters. The green and grey areas indicate the range of observed CS/GR values for Hyytiälä and Beijing, respectively. (For interpretation of the references to colour in this figure legend, the reader is referred to the Web version of this article.)

Declaration of competing interest

The authors declare that they have no known competing financial interests or personal relationships that could have appeared to influence the work reported in this paper.

Acknowledgements

We acknowledge the following projects: ACCC Flagship funded by the Academy of Finland grant number 337549, Academy professorship funded by the Academy of Finland (grant no. 302958), Academy of Finland projects no. 1325656, 316114 and 325647, Russian Mega Grant project "Megapolis - heat and pollution island: interdisciplinary hydroclimatic, geochemical and ecological analysis" application reference 2020-220-08-5835, "Quantifying carbon sink, CarbonSink+ and their interaction with air quality" INAR project funded by Jane and Aatos Erkko Foundation, European Research Council (ERC) project ATM-GTP Contract No. 742206, Samsung PM2.5 SRP, the European Union's Horizon 2020 research and innovation programme Marie Sklodowska-Curie grant agreement no. 895875 ("NPF-PANDA") and the Marie Skłodowska Curie ITN "CLOUD-MOTION" (764991) and the Arena for the gap analysis of the existing Arctic Science Co-Operations (AASCO) funded by Prince Albert Foundation Contract No 2859. Technical and scientific staff in Beijing and Hyytiälä stations are acknowledged.

Appendix A. Supplementary data

Supplementary data to this article can be found online at https://doi.org/10.1016/j.jaerosci.2021.105878.

References

Aalto, P., Hämeri, K., Becker, E., Weber, R., Salm, J., Mäkelä, J. M., Hoell, C., O'dowd, C. D., Hansson, H.-C., & Väkevä, M. (2001). Physical characterization of aerosol particles during nucleation events. *Tellus B: Chemical and Physical Meteorology, 53*.

Beck, L., Sarnela, N., Junninen, H., Hoppe, C. J. M., Garmash, O., Bianchi, F., Riva, M., Rose, C., Peräkylä, O., Wimmer, D., Kausiala, O., Jokinen, T., Ahonen, L., Mikkilä, J., Hakala, J., He, H.-U., Kontkanen, J., Wolf, K. K. E., Cappelletti, D., … Sipilä, M. (2021). Differing mechanisms of new particle formation at two arctic sites. *Geophysical Research Letters, 48*, Article e2020GL091334.

Bianchi, F., Junninen, H., Bigi, A., Sinclair, V. A., Dada, L., Hoyle, C. R., Zha, Q., Yao, L., Ahonen, L. R., Bonasoni, P., Buenrostro Mazon, S., Hutterli, M., Laj, P., Lehtipalo, K., Kangasluoma, J., Kerminen, V.-M., Kontkanen, J., Marinoni, A., Mirme, S., … Dommen, J. (2021). Biogenic particles formed in the Himalaya as an important source of free tropospheric aerosols. *Nature Geoscience, 14*, 4–9.

Bianchi, F., Tröstl, J., Junninen, H., Frege, C., Henne, S., Hoyle, C. R., Molteni, U., Herrmann, E., Adamov, A., Bukowiecki, N., Chen, X., Duplissy, J., Gysel, M., Hutterli, M., Kangasluoma, J., Kontkanen, J., Kürten, A., Manninen, H. E., Münch, S., … Baltensperger, U. (2016). New particle formation in the free troposphere: A question of chemistry and timing. *Science, 352*(6289), 1109–1112.

Brean, J., Dall'Osto, M., Simó, R., Shi, Z., Beddows, D. C. S., & Harrison, R. M. (2021). Open ocean and coastal new particle formation from sulfuric acid and amines around the Antarctic Peninsula. *Nature Geoscience*. https://doi.org/10.1038/s41561-021-00751-y

Brilke, S., Fölker, N., Müller, T., Kandler, K., Gong, X., Peischl, J., Weinzierl, B., & Winkler, P. M. (2020). New particle formation and sub-10 nm size distribution measurements during the A-LIFE field experiment in Paphos, Cyprus. *Atmospheric Chemistry and Physics, 20*, 5645–5656. https://doi.org/10.5194/acp-20-5645-2020

Cai, R., Chen, D.-R., Hao, J., & Jiang, J. (2017). A miniature cylindrical differential mobility analyzer for sub-3 nm particle sizing. *Journal of Aerosol Science, 106*, 111–119. https://doi.org/10.1016/j.jaerosci.2017.01.004

Cai, R., Yang, D., Fu, Y., Wang, X., Li, X., Ma, Y., Hao, J., Zheng, J., & Jiang, J. (2017a). Aerosol surface area concentration: A governing factor in new particle formation in beijing. *Atmospheric Chemistry and Physics, 17*, 12327–12340. https://doi.org/10.5194/acp-17-12327-2017

Cai, R. L., Yan, C., Yang, D. S., Yin, R. J., Lu, Y. Q., Deng, C. J., Fu, Y. Y., Ruan, J. X., Li, X. X., Kontkanen, J., Zhang, Q., Kangasluoma, J., Ma, Y., Hao, J. M., Worsnop, D. R., Bianchi, F., Paasonen, P., Kerminen, V. M., Liu, Y. C., … Jiang, J. K. (2021). Sulfuric acid-amine nucleation in urban Beijing. *Atmospheric Chemistry and Physics, 21*(4), 2457–2468.

Chu, B., Kerminen, V.-M., Bianchi, F., Yan, C., Petäjä, T., & Kulmala, M. (2019). Atmospheric new particle formation in China. *Atmospheric Chemistry and Physics, 19*, 115–138.

Dada, L., Chellapermal, R., Buenrostro Mazon, S., Paasonen, P., Lampilahti, J., Manninen, H. E., Junninen, H., Petäjä, T., Kerminen, V. M., & Kulmala, M. (2018). Refined classification and characterization of atmospheric new-particle formation events using air ions. *Atmospheric Chemistry and Physics, 18*, 17883–17893. https://doi.org/10.5194/acp-18-17883-2018

Deng, C., Cai, R., Yan, C., Zheng, J., & Jiang, J. (2021). formation and growth of sub-3nm particles in megacities: Impact of background aerosols. *Faraday Discussions, 226*, 348–363.

Deng, C., Fu, Y., Dada, L., Yan, C., Cai, R., Yang, D., Zhou, Y., Yin, R., Lu, Y., Li, X., Qiao, X., Fan, X., Nie, W., Kontkanen, J., Kangasluoma, J., Chu, B., Ding, A., Kerminen, V.-M., Paasonen, P., … Jiang, J. (2020). Seasonal characteristics of new particle formation and growth in urban beijing. *Environmental Science & Technology, 54*(14), 8547–8557.

Fu, Y., Xue, M., Cai, R., Kangasluoma, J., & Jiang, J. (2019). Theoretical and experimental analysis of the core sampling method: Reducing diffusional losses in aerosol sampling line. *Aerosol Science & Technology, 53*(7), 793–801. https://doi.org/10.1080/02786826.2019.1608354

Gordon, H., Kirkby, J., Baltensperger, U., Bianchi, F., Breitenlechner, M., Curtius, J., Dias, A., Dommen, J., Donahue, N. M., Dunne, E. M., Duplissy, J., Ehrhart, S., Flagan, R. C., Frege, C., Fuchs, C., Hansel, A., Hoyle, C. R., Kulmala, M., Kürten, A., … Carslaw, K. S. (2017). Causes and importance of new particle formation in the present-day and preindustrial atmospheres. *Journal of Geophysical Research - D: Atmospheres, 122*, 8739–8760.

Guo, S., Hu, M., Zamora, M. L., Peng, J., Shang, D., Zheng, J., Du, Z., Wu Shao, M., Zeng, L., Molina, M. J., & Zhang, R. (2014). Elucidating severe urban haze formation in China. *Proceedings of the National Academy of Sciences of the United States of America, 111*, 17373–17378.

Hari, P., & Kulmala, M. (2005). Station for measuring ecosystm-atmosphere relations (SMEAR II). *Boreal Environment Research, 10*, 315–322.

Hirsikko, A., Nieminen, T., Gagné, S., Lehtipalo, K., Manninen, H. E., Ehn, M., Hõrrak, U., Kerminen, V.-M., Laakso, L., McMurry, P. H., Mirme, A., Mirme, S., Petäjä, T., Tammet, H., Vakkari, V., Vana, M., & Kulmala, M. (2011). Atmospheric ions and nucleation: A review of observations. *Atmospheric Chemistry and Physics, 11*, 767–798. https://doi.org/10.5194/acp-11-767-2011

Iida, K., Stolzenburg, M. R., & McMurry, P. H. (2009). Effect of working fluid on sub-2 nm particle detection with a laminar flow ultrafine condensation particle counter. *Aerosol Science and Technology, 43*, 81–96. https://doi.org/10.1080/02786820802488194

Jiang, J., Chen, M., Kuang, C., Attoui, M., & McMurry, P. H. (2011). Electrical mobility spectrometer using a diethylene glycol condensation particle counter for measurement of aerosol size distributions down to 1 nm. *Aerosol Science and Technology, 45*(4), 510–521.

Jiang, J., Zhao, J., Chen, M., Eisele, F. L., Scheckman, J., Williams, B. J., Kuang, C., & McMurry, P. H. (2011). First Measurements of Neutral Atmospheric Cluster and 1–2 nm particle number size distributions during nucleation events. *Aerosol Science and Technology, 45*(4), ii–v.

Jokinen, T., Sipilä, M., Kontkanen, J., Vakkari, V., Tisler, P., Duplissy, E.-M., Junninen, H., Kangasluoma, J., Manninen, H. E., Petäjä, T., Kulmala, M., Worsnop, D. R., Kirkby, J., Virkkula, A., & Kerminen, V.-M. (2018). Ion induced sulfuric acid-ammonia nucleation drives particle formation in coastal Antarctica. *Sci. Adv., 4*, Article eaat9744.

Kangasluoma, J., Cai, R. L., Jiang, J. K., Deng, C. J., Stolzenburg, D., Ahonen, L. R., Chan, T., Fu, Y. Y., Kim, C., Laurila, T. M., Zhou, Y., Dada, L., Sulo, J., Flagan, R. C., Kulmala, M., Petaja, T., & Lehtipalo, K. (2020). Overview of measurements and current instrumentation for 1-10 nm aerosol particle number size distributions. *Journal of Aerosol Science, 148*, Article 105584. https://doi.org/10.1016/j.jaerosci.2020.105584, 2020.

Kangasluoma, J., Junninen, H., Lehtipalo, K., Mikkilä, J., Vanhanen, J., Attoui, M., Sipilä, M., Worsnop, D., Kulmala, M., & Petäjä, T. (2013). Remarks on ion generation for CPC detection efficiency studies in sub-3-nm size range. *Aerosol Science & Technology, 47*, 556–563. https://doi.org/10.1080/02786826.2013.773393

Kangasluoma, J., & Kontkanen, J. (2017). On the sources of uncertainty in the sub-3 nm particle concentration measurement. *Journal of Aerosol Science, 112*, 34–51.

Kangasluoma, J., Samodurov, A., Attoui, M., Franchin, A., Junninen, H., Korhonen, F., Kurtén, T., Vehkamäki, H., Sipilä, M., Lehtipalo, K., Worsnop, D. R., Petäjä, T., & Kulmala, M. (2016). Heterogeneous nucleation onto ions and neutralized ions: Insights into sign-preference. *Journal of Physical Chemistry C, 120*(13), 7444–7450.

Kerminen, V.-M., Chen, X., Vakkari, V., Petäjä, T., Kulmala, M., & Bianchi, F. (2018). Atmospheric new particle formation and growth: Review of field observations. *Environmental Research Letters, 13*, Article 103003.

Kerminen, V.-M., & Kulmala, M. (2002). Analytical formulae connecting the "real" and the "apparent" nucleation rate and the nuclei number concentration for atmospheric nucleation events. *Journal of Aerosol Science, 33*, 609–622.

Kontkanen, J., Deng, C., Fu, Y., Dada, L., Zhou, Y., Cai, J., Daellenbach, K. R., Hakala, S., Kokkonen, T. V., Lin, Z., Liu, Y., Wang, Y., Yan, C., Petäjä, T., Jiang, J., Kulmala, M., & Paasonen, P. (2020). Size-resolved particle number emissions in Beijing determined from measured particle size distributions. *Atmospheric Chemistry and Physics, 20*, 11329–11348. https://doi.org/10.5194/acp-20-11329-2020

Kontkanen, J., Järvinen, E., Manninen, H. E., Lehtipalo, K., Kangasluoma, J., Decesari, S., Gobbi, G. P., Laaksonen, A., Petäjä, T., & Kulmala, M. (2016). High concentrations of sub-3 nm clusters and frequent new particle formation observed in the Po Valley, Italy, during the PEGASOS 2012 campaign. *Atmospheric Chemistry and Physics, 16*, 1919–1935. https://doi.org/10.5194/acp-16-1919-2016

Kontkanen, J., Lehtipalo, K., Ahonen, L., Kangasluoma, J., Manninen, H. E., Hakala, J., Rose, C., Sellegri, K., Xiao, S., Wang, L., Qi, X., Nie, W., Ding, A., Yu, H., Lee, S., Kerminen, V.-M., Petäjä, T., & Kulmala, M. (2017). Measurements of sub-3 nm particles using a particle size magnifier in different environments: From clean mountain top to polluted megacities. *Atmospheric Chemistry and Physics, 17*, 2163–2187. https://doi.org/10.5194/acp-17-2163-2017

Kuang, C., Chen, M., Zhao, J., Smith, J., McMurry, P. H., & Wang, J. (2012). Size and time-resolved growth rate measurements of 1 to 5 nm freshly formed atmospheric nuclei. *Atmospheric Chemistry and Physics, 12*, 3573–3589. https://doi.org/10.5194/acp-12-3573-2012

Kulmala, M., Dada, L., Daellenbach, K. R., Yan, C., Stolzenburg, D., Kontkanen, J., Ezhova, E., Hakala, S., Tuovinen, S., Kokkonen, T. V., Kurppa, M., Cai, R., Zhou, Y., Yin, R., Baalbaki, R., Chan, T., Chu, B., Deng, C., Fu, Y., … Kerminen, V.-M. (2021). *Faraday Discussions*. https://doi.org/10.1039/dofd00078g

Kulmala, M., Kerminen, V.-M., Petäjä, T., Ding, A. J., & Wang, L. (2017). Atmospheric gas-to-particle conversion: Why NPF events are observed in megacities? *Faraday Discussions, 200*, 271–288. https://doi.org/10.1039/c6fd00257a

Kulmala, M., Kontkanen, J., Junninen, H., Lehtipalo, K., Manninen, H. E., Nieminen, T., Petäjä, T., Sipilä, M., Schobesberger, S., Rantala, P., Franchin, A., Jokinen, T., Järvinen, E., Äijälä, M., Kangasluoma, J., Hakala, J., Aalto, P. P., Paasonen, P., Mikkilä, J., … Worsnop, D. R. (2013). Direct observations of atmospheric aerosol nucleation. *Science, 339*, 943–946. https://doi.org/10.1126/science.1227385

Kulmala, M., Petäjä, T., Ehn, M., Thornton, J., Sipilä, M., Worsnop, D. R., & Kerminen, V.-M. (2014). Chemistry of atmospheric nucleation: On the recent advances on precursor characterization and atmospheric cluster composition in connection with atmospheric new particle formation. *Annual Review of Physical Chemistry, 65*, 21–37.

Kulmala, M., Petäjä, T., Nieminen, T., Sipilä, M., Manninen, H. E., Lehtipalo, K., Dal Maso, M., Aalto, P. P., Junninen, H., Paasonen, P., Riipinen, I., Lehtinen, K. E. J., Laaksonen, A., & Kerminen, V.-M. (2012). Measurement of the nucleation of atmospheric aerosol particles. *Nature Protocols, 7*, 1651–1667. https://doi.org/10.1038/nprot.2012091

Kulmala, M., Pirjola, L., & Mäkelä, J. M. (2000). Stable sulphate clusters as a source of new atmospheric particles. *Nature, 404*, 66–69.

Kulmala, M., Riipinen, I., Sipila, M., Manninen, H. E., Petaja, T., Junninen, H., dal Maso, M., Mordas, G., Mirme, A., Vana, M., Hirsikko, A., Laasko, L., Harrison, R. M., Hanson, I., Leung, C., Lehtinen, K. E. J., & Kerminen, V.-M. (2007). Toward direct measurement of atmospheric nucleation. *Science, 318*(5847), 89–92.

Kulmala, M., Vehkamäki, H., Petäjä, T., Dal Maso, M., Lauri, A., Kerminen, V.-M., Birmili, W., & McMurry, P. H. (2004). formation and growth rates of ultrafine atmospheric particles: A review of observations. *Journal of Aerosol Science, 35*, 143–176.

Lehtinen, K. E. J., Dal Maso, M., Kulmala, M., & Kerminen, V.-M. (2007). Estimating nucleation rates from apparent particle formation rates and vice-versa: Revised formulation of the Kerminen-Kulmala equation. *Journal of Aerosol Science, 38*, 988–994.

Lehtipalo, K., Kulmala, M., Sipilä, M., Petäjä, T., Vana, M., Ceburnis, D., Dupuy, R., & O'Dowd, C. D. (2010). Nanoparticles in boreal forest and coastal environment: A comparison of observations and implications of the nucleation mechanism. *Atmospheric Chemistry and Physics, 10*, 7009–7016.

Lehtipalo, K., Sipilä, M., Riipinen, I., Nieminen, T., & Kulmala, M. (2009). Analysis of atmospheric neutral and charged molecular clusters in boreal forest using pulse-height CPC. *Atmospheric Chemistry and Physics, 9*, 4177–4184. https://doi.org/10.5194/acp-9-4177-2009

Lehtipalo, K., Yan, C., Dada, L., Bianchi, F., Xiao, M., Wagner, R., Stolzenburg, D., Ahonen, L. R., Amorim, A., Baccarini, A., Bauer, P. S., Baumgartner, B., Bergen, A., Bernhammer, A.-K., Breitenlechner, M., Brilke, S., Buchholz, A., Buenrostro Mazon, S., Chen, D., … Worsnop, D. R. (2018). Multi-component new particle formation from sulfuric acid, ammonia, and biogenic vapors. *Science Adv, 12*. https://doi.org/10.1126/sciadv.aau5363. eaau5363.

Liu, Y. C., Yan, C., Feng, Z., Zheng, F., Fan, X., Zhang, Y., Li, C., Zhou, Y., Lin, Z., Guo, Y., Zhang, Y., Ma, L., Zhou, W., Liu, Z., Dada, L., Dällenbach, K., Kontkanen, J., Cai, R., Chan, T., … Kulmala, M. (2020). Continuous and comprehensive atmospheric observation in beijing: A station to understand the complex urban atmospheric environment. *Big Earth Data, 4*, 295–321.

Manninen, H. E., Nieminen, T., Asmi, E., Gagne, S., Häkkinen, S., Lehtipalo, K., Aalto, P., Vana, M., Mirme, A., Mirme, S., Hõrrak, U., Plass-Dülmer, C., Stange, G., Kiss, G., Hoffer, A., Töro, N., Moerman, M., Henzing, B., de Leeuw, G., … Kulmala, M. (2010). EUCAARI ion spectrometer measurements at 12 European sites – analysis of new particle formation events. *Atmospheric Chemistry and Physics, 10*, 7907–7927.

Manninen, H. E., Petäjä, T., Asmi, E., Riipinen, I., Nieminen, T., Mikkilä, J., Hörrak, U., Mirme, A., Mirme, S., Laakso, L., Kerminen, V.-M., & Kulmala, M. (2009). Long-term field measurements of charged and neutral clusters using Neutral cluster and Air Ion Spectrometer (NAIS). *Boreal Environment Research, 14*, 591–605.

Mirme, S., & Mirme, A. (2013). The mathematical principles and design of the NAIS - a spectrometer for the measurement of cluster ion and nanometer aerosol size distributions. *Atmos Meas Tech, 6*, 1061–1071. https://doi.org/10.5194/amt-6-1061-2013

Ohlwein, S., Kappeler, R., Joss, M, K., Künzli, N. and Hoffmann, B.: Health effects of ultrafine particles: A systematic literature review update of epidemiological evidence. International Journal of Public Health, 64, 547-559.

Rose, C., Sellegri, K., Asmi, E., Hervo, M., Freney, E., Colomb, A., Junninen, H., Duplissy, J., Sipilä, M., Kontkanen, J., Lehtipalo, K., & Kulmala, M. (2015). Major contribution of neutral clusters to new particle formation at the interface between the boundary layer and the free troposphere. *Atmospheric Chemistry and Physics, 15*, 3413–3428. https://doi.org/10.5194/acp-15-3413-2015

Rose, C., Zha, Q., Dada, L., Yan, C., Lehtipalo, K., Junninen, H., Mazon, S. B., Jokinen, T., Sarnela, N., Sipilä, M., Petäjä, T., Kerminen, V.-M., Bianchi, F., & Kulmala, M. (2018). Observations of biogenic ion-induced cluster formation in the atmosphere. *Sci. Adv., 4*(4). https://doi.org/10.1126/sciadv.aar5218

Sipilä, M., Lehtipalo, K., Kulmala, M., Petäjä, T., Junninen, H., Aalto, P. P., Manninen, H. E., Kyrö, E.-M., Asmi, E., Riipinen, I., Curtius, J., Kürten, A., Borrmann, S., & O'Dowd, C. D. (2008). Applicability of condensation particle counters to measure atmospheric clusters. *Atmospheric Chemistry and Physics, 8*, 4049–4060. https://doi.org/10.5194/acp-8-4049-2008

Sipilä, M., Sarnela, N., Jokinen, T., Henschel, H., Junninen, H., Kontkanen, J., Richters, S., Kangasluoma, J., Franchin, A., Peräkylä, O., Rissanen, M. P., Ehn, M., Vehkamäki, H., Kurtèn, T., Berndt, T., Petäjä, T., Worsnop, D., Ceburnis, D., Kerminen, V.-M., Kulmala, M., & O'Dowd, C. (2016). Molecular-scale evidence of aerosol particle formation via sequential addition of HIO_3. *Nature*. https://doi.org/10.1038/nature19314

Stolzenburg, D., Steiner, G., & Winkler, P. M. (2017). A DMA-train for precision measurement of sub-10 nm aerosol dynamics. *Atmos. Meas. Tech., 10*(4), 1639–1651. https://doi.org/10.5194/amt-10-1639-2017

Sulo, J., Sarnela, N., Kontkanen, J., Ahonen, L., Paasonen, P., Laurila, T., Jokinen, T., Kangasluoma, J., Junninen, H., Sipilä, M., Petäjä, T., Kulmala, M. and Lehtipalo, K.: Long-term measurement of sub-3 nm particles and their precursor gases in the boreal forest. Atmospheric Chemistry and Physics, 21, 695-715.

Tammet, H. (1995). Size and mobility of nanometer particles, clusters and ions. *Journal of Aerosol Science, 26*, 459–475.

Tuovinen, S., Kontkanen, J., Jiang, J., & Kulmala, M. (2020). Investigating the effectiveness of condensation sink based on heterogeneous nucleation theory. *Journal of Aerosol Science, 149*, Article 105613.

Vanhanen, J., Mikkilä, J., Lehtipalo, K., Sipilä, M., Manninen, H. E., Siivola, E., Petäjä, T., & Kulmala, M. (2011). Particle size magnifier for nano-CN detection. *Aerosol Science & Technology, 45*, 533–542.

Wimmer, D., Lehtipalo, K., Franchin, A., Kangasluoma, J., Kreissl, F., Kürten, A., Kupc, A., Metzger, A., Mikkilä, J., Petäjä, T., Riccobono, F., Vanhanen, J., Kulmala, M., & Curtius, J. (2013). Performance of diethylene glycol-based particle counters in the sub-3 nm size range. *Atmos. Meas. Tech., 6*, 1793–1804. https://doi.org/10.5194/amt-6-1793-2013

Xiao, S., Wang, M. Y., Yao, L., Kulmala, M., Zhou, B., Yang, X., Chen, J. M., Wang, D. F., Fu, Q. Y., Worsnop, D. R., & Wang, L. (2015). Strong atmospheric new particle formation in winter in urban Shanghai, China. *Atmospheric Chemistry and Physics, 15*, 1769–1781. https://doi.org/10.5194/acp-15-1769-2015

Yan, C., Yin, R., Lu, Y., Dada, L., Yang, D., Fu, Y., Kontkanen, J., Deng, C., Garmash, O., Ruan, J., Baalbaki, R., Schervish, M., Cai, R., Bloss, M., Chan, T., Chen, T., Chen, Q., Chen, X., Chen, Y., … Bianchi, F. (2021). The synergistic role of sulfuric acid, bases, and oxidized organics governing new-particle formation in Beijing. *Geophysical Research Letters, 48*, Article e2020GL091944.

Yao, L., Garmash, O., Bianchi, F., Zheng, J., Yan, C., Kontkanen, J., Junninen, H., Buenrostro Mazon, S., Ehn, M., Paasonen, P., Sipilä, M., Wang, M., Wang, X., Xiao, S., Chen, H., Lu, Y., Zhang, B., Wang, D., Fu, Q., … Wang, L. (2018). Atmospheric new particle formation from sulfuric acid and amines in a Chinese megacity. *Science, 361*, 278–281.

Yli-Juuti, T., Nieminen, T., Hirsikko, A., Aalto, P. P., Asmi, E., Hõrrak, U., Manninen, H. E., Patokoski, J., Dal Maso, M., Petäjä, T., Rinne, J., Kulmala, M., & Riipinen, I. (2011). Growth rates of nucleation mode particles in Hyytiälä during 2003−2009: Variation with particle size, season, data analysis method and ambient conditions. *Atmospheric Chemistry and Physics, 11*, 12865–12886. https://doi.org/10.5194/acp-11-12865-2011.

Yu, H., Kanawade, V. P., You, Y., Hallar, A. G., Mccubbin, I. B., Chirokova, G., Sedlacek, A. J., Springston, S. R., Wang, J., Mc-Graw, R. L., Mikkila, J., & Lee, S. H. (2014). Sub-3 nm particles observed at the coastal and continental sites in the United States. *Journal of Geophysical Research - D: Atmospheres*, 119. https://doi.org/10.1002/2013JD020841

Yu, H., Zhou, L., Dai, L., Shen, W., Dai, W., Zheng, J., Ma, Y., & Chen, M. (2016). Nucleation and growth of sub-3 nm particles in the polluted urban atmosphere of a megacity in China. *Atmospheric Chemistry and Physics, 16*, 2641–2657. https://doi.org/10.5194/acp-16-2641-2016

Zhou, Y., Dada, L., Liu, Y., Fu, Y., Kangasluoma, J., Chan, T., Yan, C., Chu, B., Daellenbach, K. R., Bianchi, F., Kokkonen, T. V., Liu, Y., Kujansuu, J., Kerminen, V.-M., Petäjä, T., Wang, L., Jiang, J., & Kulmala, M. (2020). Variation of size-segregated particle number concentrations in wintertime Beijing. *Atmospheric Chemistry and Physics, 20*, 1201–1216. https://doi.org/10.5194/acp-20-1201-2020